1 Aircraft VOC measurements

Constant, median mixing ratios of VOCs measured on the NCAR C-130 and NASA P-3B during the FRAPPÈ and DISCOVER-AQ field campaigns are used to supplement whole-air canister VOCs and further constrain the RACM2 and MCMv331 chemical models used in this study. Median mixing ratios and standard deviations of species for MOPS measurement days are shown in Table S1. Mixing ratios are calculated for only measurement points less than 1 km asl for the vicinity of Golden, CO, and a well-mixed boundary layer is assumed.

2 Model uncertainty analyses

To calculate the RACM2 uncertainty, we use a Random Sampling-High Dimensional Model Representation (RS-HDMR) technique outlined in Chen et al. (2012) and Chen and Brune (2012). Median values of all model inputs are calculated for the following two-hour time periods: 0600-0800 LT, 0800-1000 LT, 1000-1200 LT, 1200-1400 LT, and 1400-1800 LT. In total, 7 inorganic species, 32 VOC groups, 34 photolysis rates, 443 reaction rate coefficients, 615 product yields, and 168 deposition rates were randomly varied across their respective uncertainty ranges to determine the influence of input perturbations on model $P(O_3)$. Input uncertainties are outlined in Table S2. To further reduce computational time, the Morris Method is used to pre-screen model constraints, identifying roughly 50-100 of the most influential inputs on the model output, $P(O_3)$ (Morris, 1991). The $P(O_3)$ variation due to changes in influential inputs and parameters is computed using Aerodyne Research, Inc. ExploreHD software (http://www.aerodyne.com/products/explorehd), decomposing the contribution of individual model inputs on the $P(O_3)$ output. The RACM2 RS-HDMR model $P(O_3)$ uncertainties are determined as the standard deviation in calculated $P(O_3)$ divided by its mean $P(O_3)$ for each time period above (Table S4).

The MCMv331 uncertainty is calculated for the same time periods between 0600-1800 LT by perturbing model constraints one-at-a-time to both their upper or lower uncertainty limits in a local sensitivity analysis. That is, for each sensitivity run, each variable or group of variables is adjusted to their upper or lower uncertainty values while keeping all other constraints at their original values. The following input groups are perturbed one at a time to examine its effect on MCMv331-calculated $P(O_3)$: NO_x (NO_2 + NO), O_3, photolysis rates (J-values), all measured

VOCs, product yields, and reaction rate coefficients. We select and vary reaction rate coefficients and product yields that are considered to be influential from the RACM2 RS-HDMR analysis. The MCMv331 input and parameter uncertainties (1σ) for these selected parameters are shown in Table S3.

The percent differences for each sensitivity run from the MCMv331 base run are shown in Fig. S1. All upper and lower percent deviations in Fig. S1 are added in quadrature to determine total upper and lower uncertainty bounds for MCMv331 $P(O_3)$. Hourly uncertainties for MCMv331 $P(O_3)$ are averaged for each RACM2 uncertainty time period and shown in Table S4.

3 Model sensitivity studies varying HO_x and NO_x species

A number of model sensitivity studies focusing on HO_x (HO_2 + OH) and NO_x (NO_2 + NO) cycling have been conducted to assess model behavior to changes in these species. One reaction that we speculate can explain the observed discrepancy between modeled and measured HO_2, and thus modeled and measured $P(O_3)$, is the reaction described in the main text,

$$OH + NO + O_2 \longrightarrow HO_2 + NO_2 \cdot \quad \{1\}$$

We explore the effect of adding this reaction to the base case MCMv331 runs, assuming atmospheric O_2 levels and varying an effective bimolecular rate coefficient for this reaction between (3-15)x10^{-11} cm^3 molecule^{-1}s^{-1}. When this rate coefficient is adjusted to higher values (faster rate of reaction), closer agreement is seen between MOPS and modeled $P(O_3)$ diurnal patterns. Figure S2 shows the effect of varying this reaction rate coefficient.

NO_x levels were also adjusted up or down by a factor of two to assess model sensitivity to this species. While varying NO_x levels, it is clear that (as in a VOC-sensitive regime), increasing NO_x levels decrease $P(O_3)$, while lowering NO_x levels acts to increase $P(O_3)$. Sensitivity runs that increase the thermal decomposition rate of peroxynitric acid (HO_2NO_2) by a factor of 5 as in Kanaya et al. (2007) are also shown, but elevate $P(O_3)$ at all times of the day rather than in the early morning when model-measurement $P(O_3)$ discrepancies exist and are most pronounced.

4 NO_x-VOC sensitivity

To assess NO_x-VOC sensitivity in this study, we calculate the metric L_N/Q in RACM2, which represents the fraction of free radicals removed by NO_x (Kleinman et al., 2001). A L_N/Q value much greater than 0.5 represents a VOC-sensitive regime whereas a L_N/Q value much less than 0.5 represents a NO_x-sensitive regime. This metric was calculated for full-campaign data on MOPS measurement days and suggests that before 1200 LT, ozone production is VOC-sensitive where decreases in VOCs will be more effective in decreasing $P(O_3)$ and subsequent NO_x decreases will act to increase $P(O_3)$ (Fig. S3). After 1200 LT, $P(O_3)$ is primarily NO_x sensitive, where decreasing NO_x will linearly decrease $P(O_3)$. With the added OH + NO $(+O_2) \rightarrow HO_2 + NO_2$ reaction ($k_{OH+NO} = 15\text{x}10^{-11}\text{cm}^3\text{molec}^{-1}\text{s}^{-1}$), $P(O_3)$ shifts to a NO_x sensitive regime approximately one to two hours earlier in the day, suggesting that there is a longer time period in the morning where $P(O_3)$ is NO_x-sensitive, similar to conclusions drawn from the MOPS measurements.

References

Atkinson, R., 1991: Kinetics and Mechanisms of the Gas-Phase Reactions of the NO3 Radical with Organic Compounds. *Journal of Physical and Chemical Reference Data*, **20 (3)**, 459–507, doi:10.1063/1.555887, URL http://scitation.aip.org/content/aip/journal/jpcrd/20/3/10.1063/1.555887.

Atkinson, R., and S. M. Aschmann, 1989: Rate constants for the gas-phase reactions of the OH radical with a series of aromatic hydrocarbons at 296 ± 2 K. *Int. J. Chem. Kinet.*, **21 (5)**, 355–365, doi:10.1002/kin.550210506, URL http://onlinelibrary.wiley.com/doi/10.1002/kin.550210506/abstract.

Atkinson, R., and Coauthors, 2006: Evaluated kinetic and photochemical data for atmospheric chemistry Volume II: gas phase reactions of organic species. *Atmos. Chem. Phys.*, **6 (11)**, 3625–4055, doi:10.5194/acp-6-3625-2006, URL http://www.atmos-chem-phys.net/6/3625/2006/.

Chen, S., and W. H. Brune, 2012: Global sensitivity analysis of ozone production and O3-NOx-VOC limitation based on field data. *Atmospheric Environment*, **55**, 288–296, doi:10.1016/j.atmosenv.2012.03.061.

Chen, S., W. H. Brune, O. O. Oluwole, C. E. Kolb, F. Bacon, G. Li, and H. Rabitz, 2012: Global sensitivity analysis of the regional atmospheric chemical mechanism: an application of random sampling-high dimensional model representation to urban oxidation chemistry. *Environmental science & technology*, **46 (20)**, 11 162–11 170, doi:10.1021/es301565w, PMID: 22963531.

Gao, D., W. R. Stockwell, and J. B. Milford, 1995: First-order sensitivity and uncertainty analysis for a regional-scale gas-phase chemical mechanism. *J. Geophys. Res.*, **100 (D11)**, 23 153–23 166, doi:10.1029/95JD02704, URL http://onlinelibrary.wiley.com/doi/10.1029/95JD02704/abstract.

Kanaya, Y., and Coauthors, 2007: Urban photochemistry in central Tokyo: 1. Observed and modeled OH and HO2 radical concentrations during the winter and summer of 2004. *J. Geophys. Res.*, **112 (D21)**, D21 312, doi:10.1029/2007JD008670, URL http://onlinelibrary.wiley.com/doi/10.1029/2007JD008670/abstract.

Kleinman, L. I., P. H. Daum, Y.-N. Lee, L. J. Nunnermacker, S. R. Springston, J. Weinstein-Lloyd, and J. Rudolph, 2001: Sensitivity of ozone production rate to ozone precursors.

Morris, M. D., 1991: Factorial sampling plans for preliminary computational experiments. *Technometrics*, **33 (2)**, 161–174.

Sander, S., and Coauthors, 2011: Chemical Kinetics and Photochemical Data for Use in Atmospheric Studies, Evaluation No. 17. JPL Publication 10-6. URL http://jpldataeval.jpl.nasa.gov.

Table S 1: Median mixing ratios and standard deviations of all aircraft species measured in the vicinity of Golden, CO for MOPS measurement days. Constant, median values of these species supplement the canister VOC measurements in both MCMv331 and RACM2.

VOC name	Mixing ratio (ppbv)	σ (ppbv)
acetaldehyde	1.32	0.72
acetone	3.51	1.02
HCHO	1.78	0.66
nitric acid	1.38	0.54
MEK	0.28	0.23
methanol	7.46	3.39
MVK/methacrolein[a,b]	100	50.8
acetic acid	0.40	0.38
PAN[a]	760	370
PPN[a]	110	60.0
H_2O_2	1.90	0.77
CH_3OOH	4.48	1.78
HCOOH	1.28	0.34
ethanol	1.00	1.09
camphene[a]	2.20	4.40
d-limonene/3-carene[b]	1.70	3.30

[a]In parts per trillion by volume (pptv)

[b]Methyl vinyl ketone and methacrolein are measured together; equal parts of each species is assumed in measurement. D-limonene/3-carene is grouped as limonene in MCMv331 and RACM2.

Table S 2: RACM2 RS-HDMR model input uncertainties adapted and estimated from Chen and Brune (2012) and modified for this study.

Number	Model Input	Uncertainty (1σ,%)
3	*Meteorological parameters:*	≤ 10
7	*Inorganics:*	
	Lowest: CO, CO_2	5
	Highest: O_3,NO_x	10
32	*VOC Groups:*	
	Lowest: ethene, ethane	3
	Highest: organic nitrates	>100
	JNO_2	40[a]
33	TUV photolysis rates	40[a]
443	*Reaction rate coefficients*	
	Inorganic reactions:	
	Lowest: OH + H_2	5[b]
	Highest: inorganics + NO_3,	42[b,d]
	HONO + OH, NO + O^3P	
	Organic + OH:	
	Lowest: ethane, ethanol, methanol	10[b]
	Highest: ISO intermediate reactions	75[a]
	Organics + NO_3	
	Lowest: α-pinene	15[d]
	Highest: DIEN (1,3-butadiene)	133[d]
	Organics + O_3	
	Lowest: ISO	19[c]
	Highest: isoprene nitrates, MOBA	75[a]
	Peroxy radical + NO	75[f]
	exceptions: ethene, CH_3O_2,	144[b]
	TOL, unsaturated and aromatic aldehydes	
	and benzaldehyde	
	RO_2 + RO_2 or HO_2	18-75[b,f]
	PAN chemistry	18-27[b]
615	*Product yields*	10-27[e]

[a]Estimated
[b]NASA JPL (Sander et al., 2011)
[c]IUPAC
[d]Atkinson (1991)
[e]Gao et al. (1995) and references therein
[f]Estimated by Chen and Brune (2012)

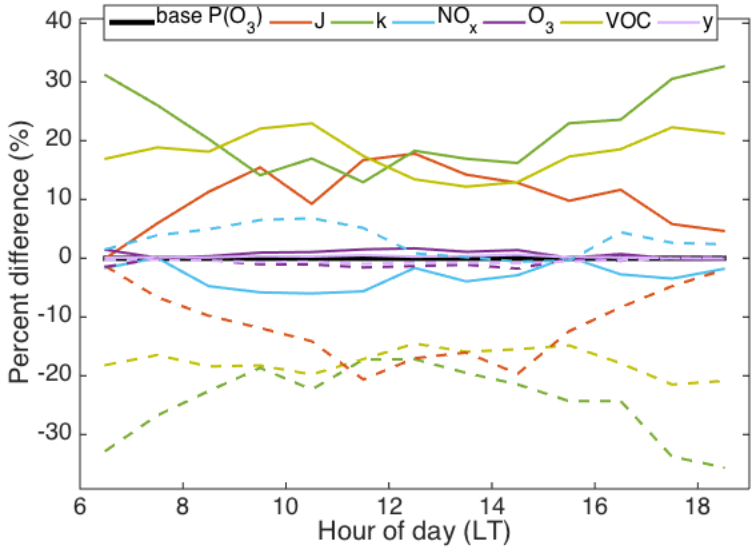

Figure S 1: MCM uncertainty analysis. Percent difference from base $P(O_3)$ calculated by increasing or decreasing the following parameters by their 1σ uncertainty levels: photolysis rates (J), select reaction rate coefficients (k), $NO_x = NO_2 + NO$, O_3, all measured VOCs, and select product yields (y). Solid (dashed) lines represent the percent difference from the base MCMv331 $P(O_3)$ run when each species is set to its upper (lower) limit.

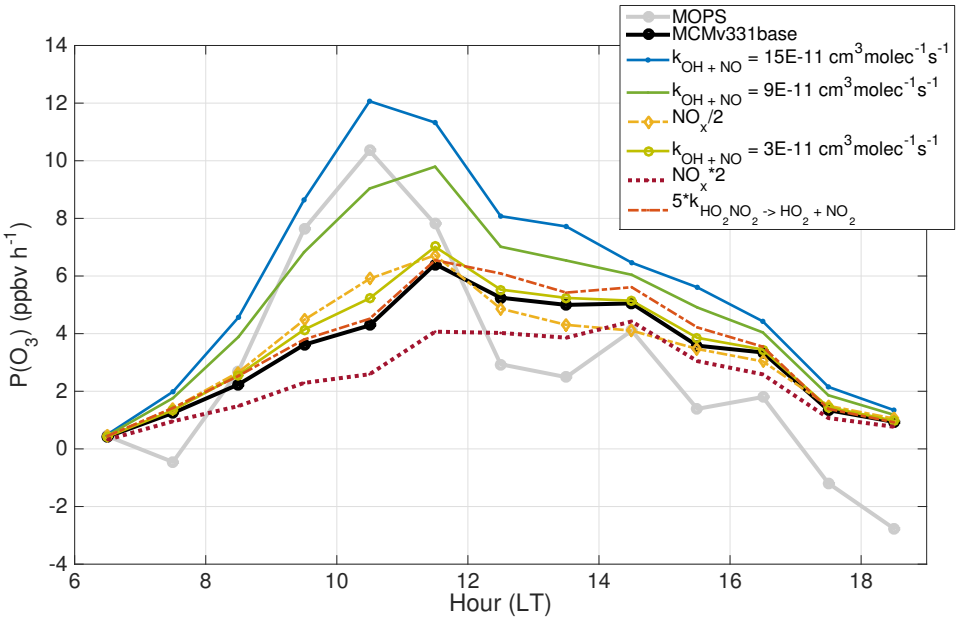

Figure S 2: Model sensitivity studies involving the possible missing reaction of OH plus NO yielding HO_2 and NO_2, and other sensitivity studies varying NO_x by a factor of two and increasing the thermal decomposition rate of peroxynitric acid by a factor of 5. Model case studies are compared to the median MCMv331 base case $P(O_3)$ as well as the MOPS $P(O_3)$.

Table S 3: Summary of select reaction rates and product yields varied for MCMv331 uncertainty analysis. Names of species are listed according to the RACM2 naming convention. Select reaction rates and product yields were varied all at once with all other constraints held at their original values.

Rate coefficient	Uncertainty (%, 1σ)	Product yield[e]	Uncertainty (%, 1σ)
k_{OH+NO_2}	27[b]	Y(EPX + O_3 → HO_2)	27
k_{HO_2+NO}	14[b]	Y(CH_3OOH + OH → HCHO + OH)	18
$k_{O^1D+H_2O}$	8[b]	Y(ISOP + NO → HO_2)	27
k_{ACO_3+NO}	42[b]	Y(HC3P + NO → NO_2)	27
k_{PAN}	18[b]	Y(XY2 → XYLP + HO2)	27
k_{PPN}	27[b]	Y(TR2 → products)	27
k_{RCO_3+NO2}	27[b]		
k_{OH+ACD}	5[b]		
k_{RCO_3+NO}	42[b]		
k_{EPX+O_3}	75[a]		
k_{XYO+OH}	14[d]		
$k_{CH_3OOH+OH}$	40[b]		
$k_{OH+HCHO}$	14[b]		
$k_{XYM,XYP+OH}$	20[d]		
k_{ISO+OH}	10[c]		
k_{ETE+OH}	18[b]		
$k_{ACO_3+NO_2}$	18[b]		

[a]Chen and Brune (2012)
[b]NASA JPL (Sander et al., 2011)
[c]Atkinson et al. (2006)
[d]Atkinson and Aschmann (1989)
[e]Gao et al. (1995)

Table S 4: Golden, CO RACM2 and MCMv331 model relative uncertainties (1σ) between 0600 and 1800 local time.

Time of day (LT)	0600-0800	0800-1000	1000-1200	1200-1400	1400-1800
RACM2 Uncertainty (%)	30	33	31	28	28
MCMv331 Uncertainty (%)	33	30	30	28	32

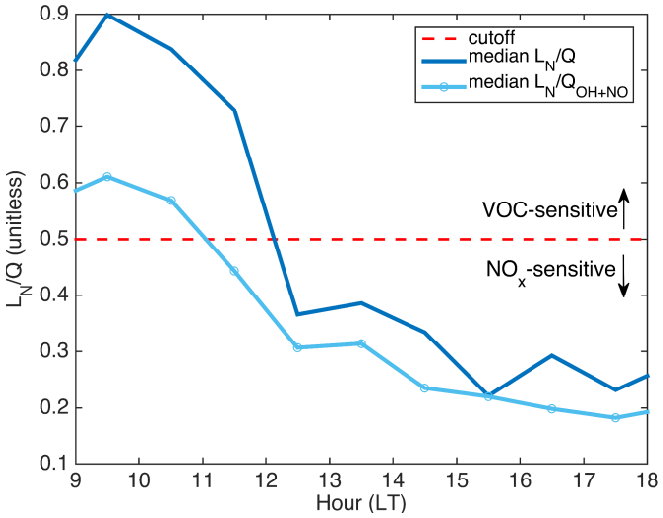

Figure S 3: Total median L_N/Q, representing the fraction of free radicals removed in the atmosphere by NO_x. L_N/Q higher than 0.5 is considered to be within a VOC-sensitive regime, whereas L_N/Q less than 0.5 is considered to be in a NO_x-sensitive regime. Also shown is the L_N/Q for RACM2 with the OH + NO (+ O_2) $\rightarrow$ HO_2 + NO_2 reaction added.